Lawrence Berkeley National Laboratory

Title
Impact of Helical Chain Shape in Sequence-Defined Polymers on Polypeptoid Block Copolymer Self-Assembly

Permalink
https://escholarship.org/uc/item/62d0w7q0

Journal
Macromolecules, 51(5)

ISSN
0024-9297

Authors
Davidson, Emily C
Rosales, Adrianne M
Patterson, Anastasia L
et al.

Publication Date
2018-03-13

DOI
10.1021/acs.macromol.8b00055

Peer reviewed

Impact of Helical Chain Shape in Sequence-Defined Polymers on Polypeptoid Block Copolymer Self-Assembly

Emily C. Davidson,[†] Adrianne M. Rosales,[§] Anastasia L. Patterson,[‡] Boris Russ,[§] Beihang Yu,[†] Ronald N. Zuckermann,[§] and Rachel A. Segalman*,[†,‡]

[†]Department of Chemical Engineering and [‡]Materials Department, University of California, Santa Barbara, Santa Barbara, California 93106, United States

[§]Molecular Foundry, Lawrence Berkeley National Laboratory, Berkeley, California 94720, United States

S *Supporting Information*
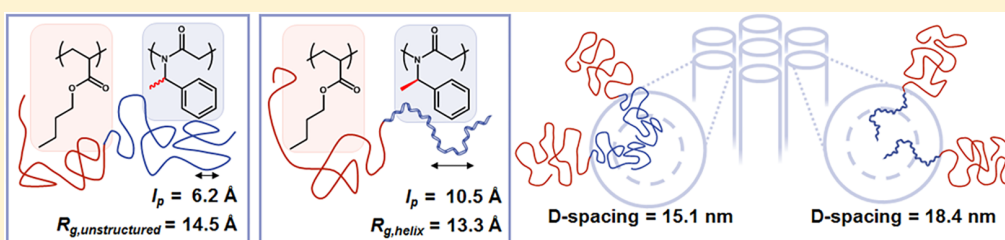
ABSTRACT: Controlling the self-assembly of block copolymers with variable chain shape and stiffness is important for driving the self-assembly of functional materials containing nonideal chains as well as for developing materials with new mesostructures and unique thermodynamic interactions. The polymer helix is a particularly important functional motif. In the helical chain, the traditional scaling relationships between local chain stiffness and space-filling properties are not applicable; this in turn impacts the scaling relationships critical for governing self-assembly. Polypeptoids, a class of sequence-defined peptidomimetic polymers with controlled helical secondary structure, were used to systematically investigate the impact of helical chain shape on block copolymer self-assembly in a series of poly(*n*-butyl acrylate)-*b*-polypeptoid block copolymers. Small-angle X-ray scattering (SAXS) of the bulk materials shows that block copolymers form hexagonally packed cylinder domains. By leveraging sequence control, the polypeptoid block was controlled to form a helix only at the part either adjacent to or distant from the block junction. Differences in domain size from SAXS reveal that chain stretching of the helix near the block junction is disfavored, while helical segments at the center of cylindrical domains contribute to unfavorable packing interactions, increasing domain size. Finally, temperature-dependent SAXS shows that helix-containing diblock copolymers disorder at lower temperatures than the equivalent unstructured diblock copolymers; we attribute this to the smaller effective *N* of the helical structure resulting in a larger entropic gain upon disordering. These results emphasize how current descriptions of rod/coil interactions and conformational asymmetry for coil polymers do not adequately address the behavior of chain secondary structures, where the scalings of space-filling and stiff—elastic properties relative to chain stiffness deviate from those of typical coil, semiflexible, and rodlike polymers.

INTRODUCTION

As new block copolymers are developed that contain nontraditional polymer segments, many are expected to have backbones of variable stiffness and/or secondary chain structures. Understanding how differences in the local stiffness, shape, and relative space-filling characteristics of these molecules impact self-assembly will enable molecular design that will in turn lead to controlled phase behavior and potentially the stabilization of new phases. Secondary structures in particular introduce nonidealities in chain trajectory that are not accounted for by current models; the chain itself no longer follows a random walk. In this work, sequence-defined polymers (polypeptoids) are leveraged which can be manipulated to form either an unstructured coil or a helical secondary structure depending on the sequence and chirality of the side chains. These polypeptoids are incorporated into block

copolymers, allowing the impact of helical secondary structure on self-assembly to be directly examined without changing backbone chemistry.

Local chain stiffness is connected to self-assembly via its effect on local enthalpic interactions, its effects on resistance to deformations of conformation, and its effect on how much space the polymer chain fills. In considering the impact of chain shape and chain stiffness, the length of the entire chain is termed the contour length L_C, while the persistence length l_p defines the local chain stiffness and is the distance along the chain contour over which correlation in direction is maintained. In other words, from a given starting point along the chain

where the chain is traveling in a certain direction, it retains some "memory" of that direction for a distance l_p along the chain. When L_C is significantly longer than l_p ($L_C > \sim 10 l_p$) the chain is well-described as a Gaussian coil; when it is on the order of the persistence length ($L_C \sim l_p$), the chain is semiflexible, while chains with a contour length that is long relative to the persistence length ($L_C \ll l_p$) can be described as rodlike.[1] This description emphasizes that persistence length alone does not describe the chain characteristics. While two chains can have identical contour lengths and chain conformation (for example, both are Gaussian chains), the chain with the larger l_p will also fill more space (larger radius of gyration, R_g).

The conformational asymmetry of a block copolymer is fundamentally related to the relative chain stiffness of the two constituent polymer chains, which is in turn parametrized by the relative persistence lengths of those chains.[2,3] If one chain (of material A) is locally considerably stiffer than the other (B), the stability of phases with curved interfaces increases for volume fractions $f_A < 1/2$.[2,3] Further, there is evidence that conformational asymmetry can expand the window of accessibility for phases near the critical point such as the bicontinuous gyroid phase and Frank–Kaspar phases, in addition to related long-lived metastable phases.[2,4] Past work on conformational asymmetry has raised important questions: in particular, are the effects of conformational asymmetry on self-assembly primarily entropic or enthalpic in nature?[5] Theoretical work predicts an entropic conformational effect on self-assembly arising from how conformational asymmetry changes the space-filling nature of chains and therefore the relative penalties for chain stretching and deformation.[6,7] In addition, there is the possibility that the origin of conformational asymmetry's role lies in an enthalpic effect: that changing the stiffness of a chain impacts the effective coordination number of each polymer unit, thus impacting the value of χ between the chains.[5]

The role of conformational asymmetry has been considered extensively for Gaussian coils—polymers where variations in stiffness translate directly to variations in space filling. For diblock copolymers composed of two Gaussian coils, a conformational asymmetry parameter has been defined, which describes the relative space-filling characteristics of the two polymer chains and relates it to the relative chain stiffnesses. In this formalism a conformational symmetry parameter β describes how condensed or expanded a polymer chain is, where $\beta^2 = R_g^2/V$, and R_g is the radius of gyration of the chain and V is the volume occupied by a single chain. For a polymer coil, $\beta^2 = a^2/(6v)$ where a is the polymer statistical segment length and v is the segment volume. Thus, for a coil–coil block copolymer, the conformational asymmetry parameter $\varepsilon = \beta_A^2/\beta_B^2$ is equal to a_A^2/a_B^2 as long as the two chains have been normalized to the same reference volume, allowing the conformational asymmetry to be directly related to the relative stiffness of the two blocks.[2] Notably, as defined $\varepsilon = a_A^2/a_B^2$ will not directly correspond to $l_{p,A}^2/l_{p,B}^2$ unless the chains have identical Kuhn segment volumes; the statistical segment lengths of each block cannot simultaneously correspond to Kuhn statistical segment lengths (where $a = l_p/2$) and be normalized to the same reference volume. Conformational asymmetry effects have been less readily considered for polymers adopting nonideal shapes. In particular, the helix, an important structural motif in both biological and synthetic polymers, is locally stiff relative to unstructured polymers (in fact, helix-forming

moieties have displayed liquid crystalline interactions).[8,9] The local stiffness and defined helical chain conformation are expected to have significant conformational entropic and enthalpic effects; however, the deviation of the chain conformation from a Gaussian chain is expected to significantly change the ramifications of these effects on block copolymer self-assembly.

In addition to deviations from ideal conformational asymmetry effects, polymer chains that adopt secondary structures deviate from the standard description of persistence length. For example, in a helix-forming polymer, the chain has a short bending radius as it forms the turns of the helix. Despite this, the helical secondary structure enables the chain to maintain correlation over long distances, resulting in a larger helix persistence length ($l_{p,helix}$) and stiffness than the unstructured chain. Essentially, given an initial vector direction along the chain contour, the projection onto the helix contour will lose correlation over $l_{p,helix}$ (Figure 1). The contour length
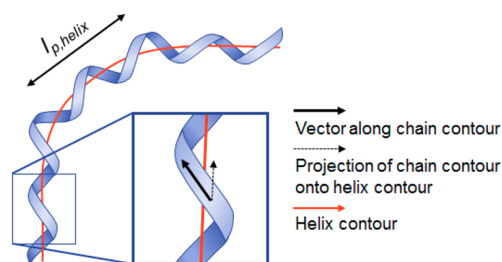

Figure 1. In a helical secondary structure the chain itself does not follow a random walk but rather forms the turns of the helix. The helix itself, however, will have some rigidity which may be described by a persistence length, $l_{p,helix}$. For an initial vector direction of the chain (black solid arrow), the projection (black dashed arrow) onto the helix contour (red solid arrow) loses correlation over distance $l_{p,helix}$.

of the helix ($L_{C,helix}$) is the sum of all projections of the chain vector along the helix contour (sum along dashed vector, Figure 1); this is in contrast to the contour length of the constituent chain. If the helix is more rodlike than the constituent chain ($l_{p,helix}/L_{C,helix}$ larger than $l_{p,chain}/L_{C,chain}$), the number of available chain configurations is expected to decrease. Because of the compact nature of the helix ($L_{C,helix} < L_{C,chain}$), the coordination number per monomer is expected to be less for the helix than for the equivalent unstructured chain, despite the more rodlike character of the helix. Essentially, local chain stiffness, coordination number per monomer, space filled (R_g), and the number of available chain configurations scale differently in secondary structures than in chains following random walk statistics. This change in scaling is expected to have significant impacts on the forces driving block copolymer self-assembly.

The polymer helix is significant both as a structural motif and for its integral role in polymer functionality. Helical architectures are essential to the structure of proteins and DNA and are known to impact their material properties, as in the case of helical fibrils of collagen.[10] Molecular helices are also found in synthetic polymers;[11–14] however, while biological polymers tend to form helices due to hydrogen-bonding interactions, synthetic polymers tend to form helices as a result of chiral interactions.[15] The physics of a helical wormlike chain have been described due to the ubiquity of helical polymers.[16–20] A number of synthetic helical polymers have the ability to sense chiral molecules and respond via a change in

conformation, therefore displaying potential for use as molecular sensors.[8,21−25] Incorporating chiral helical polymers into block copolymers provides the opportunity to not only incorporate the unique functionalities of helices into block copolymer nanostructures but also control higher levels of structure in self-assembled systems. For example, in block copolymers of polystyrene-*b*-poly(isocyano-L-alanine-L-alanine) (PS-*b*-PIAA), the molecular chirality of the isocyanodipeptide block informed the chirality of a self-assembled supramolecular helix in solution;[26] similarly, polystyrene-*b*-poly(L-lactide) (PS-*b*-PLLA) block copolymers in bulk give rise to a hexagonally packed helical phase that is not observed in the corresponding achiral system.[27−29] These studies point to the important role that secondary structure can play in self-assembly.

This work examines the self-assembly of diblock copolymers which are chemically identical but have tunable secondary structure. We leverage solid-phase synthesis of polypeptoids—a class of polymers with controlled side chain identity similar to polypeptides, but lacking backbone chirality and hydrogen bonding—making them an ideal model system for highly controlled polymer studies.[30,31] By incorporating chiral side chains, polypeptoids can be induced to form a helical secondary structure[32−35] while polypeptoids with randomly incorporated, racemic side chains remain unstructured.[36] Helical conformations have been confirmed via a combination of circular dichroism,[32,37] 2-D NMR,[33] and crystallography.[38,39] Further, we incorporate the polypeptoid helix at specific locations along the chain backbone—specifically examining the role of chain stretching at the edges of microdomains versus chain packing in the core of microdomains. Poly(*n*-butyl acrylate)-*b*-polypeptoid block copolymers in which the polypeptoid chains contain *N*-(1-phenylethyl)glycine moieties of controlled chirality form chiral secondary structures. These helical secondary structures resist chain stretching at the block interface but increase domain size when in the cylindrical core of domains. Further, block copolymers with helical structures disorder at lower temperatures than those with an unstructured chain due to an increased entropic gain upon disordering. This work emphasizes the importance of considering how conformational asymmetry manifests in secondary structures, where chain stiffness, space-filling, coordination, and conformational effects do not follow the known scalings of chains following random-walk statistics.

■ EXPERIMENTAL METHODS

Synthesis of Azide-Terminated Poly(*n*-butyl acrylate). Atom transfer radical polymerization (ATRP) was used to synthesize poly(*n*-butyl acrylate) with a bromine end group. The initiator (methyl 2-bromopropionate), solvent (anhydrous anisole), and catalyst (copper-(I) bromide) were used as received. Butyl acrylate monomer and the ligand *N,N,N′,N′,N″*-pentamethyldiethylenetriamine (PMDETA) were filtered over basic alumina before use. All were purchased from Sigma-Aldrich. In a reaction flask, the following were combined: 0.179 mmol of initiator, 0.067 mmol of PMDETA, 34.7 mmol of butyl acrylate, 0.067 mmol of Cu(I)Br, and 2 mL of anisole. The reaction mixture was degassed by three freeze−pump−thaw cycles and then heated in an oil bath at 80 °C for 6 h under nitrogen. Residual copper was removed by filtering the product through basic alumina, and the reaction mixture was precipitated into cold methanol (over dry ice). The resulting bromine-terminated poly(*n*-butyl acrylate) (0.071 mmol) was dissolved in dimethylformamide (DMF) (25 mL), and 1.5 mol equiv of sodium azide was added. The reaction mixture was stirred overnight at room temperature. The polymer was then precipitated in cold methanol and dried under vacuum at 50 °C to remove residual DMF.

Synthesis of Alkyne-Terminated Polypeptoids. Polypeptoids were synthesized on a custom robotic synthesizer or a commercial Aapptec Apex 396 robotic synthesizer according to previously published methods using commercially available amine submonomers (Figure 2).[40] Bromoacetylation steps were performed twice to enable

N*R*pe
N-(*R*-1-phenylethyl)glycine

Nmb
N-[(±)-1-phenylethyl)glycine]

Nme
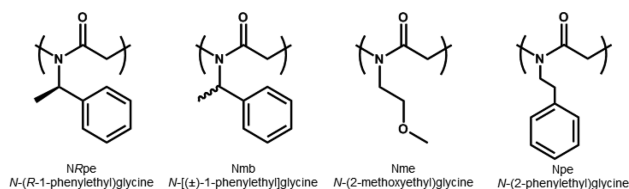*N*-(2-methoxyethyl)glycine

Npe
N-(2-phenylethyl)glycine

Figure 2. Repeat units incorporated in polypeptoid sequences include a homochiral *N*-(*R*-1-phenylethyl)glycine used to direct structure to form helical blocks (Chir*RX*, where *X* is the total number of monomers), the racemic form of the same unit, *N*-(±-1-phenylethyl)-glycine, used to form unstructured blocks (Rac*X*), a (2-methoxyethyl)-glycine spacer, and an achiral repeat unit, *N*-(2-phenylethyl)glycine, also used to form unstructured blocks (Achir*X*). Exact polypeptoid sequences can be found in Supporting Information Table 1.

high yields of desired product. The N-terminus of all polypeptoids were functionalized with an alkyne group by installing an *N*-propargylglycine monomer followed by acetylation on the resin and purification as previously described.[41] Molecular weights of the polypeptoids were determined using an Applied Biosystems 4800 series MALDI-TOF. MALDI samples were prepared using a 1:1 ratio of polypeptoid in acetonitrile (0.5 mg/mL) to 1,8,9-anthracenetriol (10 mg/mL in THF). The exact polypeptoid sequences investigated in this work are shown in Supporting Information Table 1. The sequence was chosen to be composed of repeats of a known helix-forming hexamer.[32,34,35]

Synthesis of Polypeptoid-*b*-Poly(*n*-butyl acrylate) Block Copolymers. The block copolymers were synthesized by azide−alkyne coupling using the procedure described previously (Supporting Information Scheme 1).[41] Upon completion of the reaction, the polymer was precipitated twice in cold methanol/water mixtures and centrifuged at 4 °C to collect the product. Materials were further purified by (1) dissolving in acetonitrile followed by (2) adding water dropwise until the desired product precipitated while the polypeptoid homopolymer remained in solution. This product was collected by centrifugation. Characteristics of all block copolymers are listed in Table 1.

Gel Permeation Chromatography (GPC). The molecular weights and dispersities of the poly(*n*-butyl acrylate) homopolymers were measured on a Malvern triple detector gel permeation chromatography system using Waters Styragel columns. Refractive index traces were used for molecular weight determination using polystyrene calibration standards (Polymer Laboratories) and were collected in 30 °C tetrahydrofuran with a flow rate of 1 mL/min. Representative GPC traces for the synthesized block copolymers are shown in Supporting Information Figure 1.

Circular Dichroism (CD). Solution CD measurements (Supporting Information Figure 1) were performed on a J-185 CD spectrometer (Jasco Inc.). Stock polypeptoid solutions were prepared in tared vials using 5 mg/mL of polypeptoid powder in acetonitrile. The stock solutions were diluted to a concentration of 0.1 mg/mL for acquiring CD spectra. CD spectra were collected using a quartz cell (Hellma USA) with a path length of 1 mm. A scan rate of 50 nm/min was used from 180 to 260 nm, and three measurements were averaged for each compound. Solid-state CD samples (Supporting Information Figure 2) were prepared by drop-casting polypeptoid homopolymer and polypeptoid-containing block copolymers from a tetrahydrofuran solution onto quartz discs. Discs were dried in air and then under vacuum overnight to remove residual solvent. Measurements were performed on a Jasco J-1500 spectrometer from 190 to 260 nm.

Small-Angle X-ray Scattering (SAXS). Samples were prepared by using a spatula at room temperature to fill a 1 mm thick aluminum

Table 1. Block Copolymers Used in This Study

block copolymer	composition	$M_{n,peptoid}$ (kDa)	$\varphi_{peptoid}$[a]	D (nm)	ODT[b] (°C)	morphology[c]
PnBA-*b*-Rac24	coil-*b*-unstructured	3470	0.18	N/A	N/A	DIS
PnBA-*b*-ChirR24	coil-*b*-helix	3470	0.18	N/A	N/A	DIS
PnBA-*b*-Achir36	coil-*b*-unstructured	5128	0.25	14.5		HEX
PnBA-*b*-Rac36	coil-*b*-unstructured	5128	0.25	15.1	120	HEX
PnBA-*b*-ChirR36	coil-*b*-helix	5128	0.25	18.4	115	HEX
PnBA-*b*-(ChirR18-*b*-Rac18)	coil-*b*-(helix-*b*-unstructured)	5128	0.25	16.4		HEX
PnBA-*b*-(Rac18-*b*-ChirR18)	coil-*b*-(unstructured-*b*-helix)	5128	0.25	18.6		HEX
PnBA-*b*-Rac48	coil-*b*-unstructured	6786	0.31	18.0	150	HEX
PnBA-*b*-ChirR48	coil-*b*-helix	6786	0.31	22.0	136	HEX
PnBA-*b*-Rac54	coil-*b*-unstructured	7615	0.33	19.7	201	HEX
PnBA-*b*-ChirR54	coil-*b*-helix	7615	0.33	25.0	171	HEX

[a]PnBA block has M_n = 14 000 kDa and $Đ$ = 1.11 for all diblock copolymers, as determined by GPC using PS standards. Volume fraction $\varphi_{polypeptoid} = M_n^{peptoid}/1.18/(M_n^{peptoid}/1.18 + M_n^{PnBA}/1.08)$. [b]ODTs were only measured for helical versus unstructured block copolymer pairs with 36, 48, and 54 polypeptoid units. [c]DIS = disordered; HEX = hexagonally packed cylinders.

washer with the soft poly(*n*-butyl acrylate)-containing block copolymer. One side of the sample washer was glued to a Kapton window with high temperature stable silicone adhesive (Dow Corning), and the entire sample cell was annealed in a vacuum oven (10^{-9} Torr) at 130 °C for 24 h. After annealing, a second Kapton window was glued to the washer to completely seal the polymer sample.

SAXS was conducted at the Advanced Light Source (ALS, beamline 7.3.3) and at the Stanford Synchrotron Radiation Lightsource (SSRL, previous beamline 1-4). At the ALS, the beamline was configured with an X-ray wavelength of λ = 1.240 Å and focused to a spot size of 50 by 300 μm. Two-dimensional scattering patterns were collected on a Pilatus 100k detector. At SSRL, the beamline was configured with an X-ray wavelength of λ = 1.488 Å and focused to a 0.5 mm diameter spot. A single quadrant of a two-dimensional scattering pattern was collected on a CCD detector with an active area of 25.4 mm by 25.4 mm. Calibration using silver behenate standards, radial averaging, and scattering intensity corrections were performed using the Nika package for Igor Pro.[42]

Transmission Electron Microscopy (TEM). Thin film block copolymer samples were prepared by spin-coating thin films (~100 nm) from THF onto silicon nitride (Ted Pella, 50 nm thick) and annealing in a vacuum oven overnight at 130 °C. After annealing, the samples were selectively stained with RuO₄ vapor (Electron Microscopy Sciences, 0.5% aqueous solution) for 10 min prior to characterization. TEM imaging was conducted on a JEOL JEM-2100 microscope at an operating voltage of 200 kV. Additional 100 nm thick samples were cryo-microtomed with a Leica UC7 Ultramicrotome with FC7 cryo attachment and collected directly from the dry diamond knife. Thin sections were places on CF300 amorphous carbon-coated Cu grids from Electron Microscopy Sciences and stained with RuO₄. These samples displayed significant deformation due to cryo-microtoming, but minority polypeptoid sections were stained dark, confirming that RuO₄ selectively stains polypeptoid domains, likely via the aromatic ring in the phenylethyl moiety (Supporting Information Figure 7).

RESULTS AND DISCUSSION

The impact of secondary structure on block copolymer self-assembly was investigated by examining cylindrical assembled structures in a series of diblock copolymers in which one block has a precisely controlled helical or unstructured coil conformation. Prior works have emphasized that stiffness and chain shape can have important impacts on self-assembly. Here, this relationship is examined in a polypeptoid system that controllably forms helical secondary structures. Further, the secondary structure formation is determined only by the choice of chiral versus racemic side chains. While the bending radius (local stiffness) of the chain forming the helix remains quite short, the helix itself has a longer persistence length than that of the unstructured chain.[36] This behavior, in which the helix becomes stiff relative to the unstructured chain, yet becomes less space-filling (smaller R_g), emphasizes that standard descriptions of conformational asymmetry do not adequately describe secondary structures such as helices. The helical chain shape and the placement of helical segments relative to the microdomain interface are found to have significant impacts on the final structure due to the specific impacts of space-filling, stretching, and packing interactions.

Chiral Side Chains Induce Helical Chain Shape. Here, in order to directly investigate the impact of secondary structure on self-assembly, a system was chosen in which the secondary structure could be tuned with nearly identical backbone and side chain chemistry. Previous work on polypeptoid polymers has shown that polypeptoids can be induced into a helical conformation by choosing primarily bulky, chiral side chains of the identical chirality; the equivalent polypeptoid with a racemic mix of side chains remains unstructured. In particular, by incorporating at least 50% of monomers as *N*-(*R*-1-phenylethyl)glycine, the polymer is induced into the helical conformation;[32,34,35] if a racemic combination of side groups is used instead (stoichiometric amounts of *R*- and (*S*-1-phenylethyl)glycine), the polymer retains an unstructured conformation.[36] Importantly, this method of sterically inducing the helical conformation is remarkably stable across a range of solvents and temperatures in solution and may form entropically stabilized helices (unlike hydrogen-bond-stabilized helices, which transition to an unstructured state above a critical temperature).[34,43] This remarkably environment-independent and stable helix makes it ideal for bulk studies. Indeed, circular dichroism measurements of this polypeptoid in a solid-state thin film shows that the ellipticity signal observed in solution is maintained in the solid-state (Supporting Information Figure 3). In addition, by choosing a material with secondary structure arising from side-chain chirality, these materials gain a degree of synthetic tunability that materials with main-chain chirality (such as polypeptides and PLLA) cannot. By directly changing the side chain identity for a single backbone chemistry, both analogues of helical materials with racemic side chains that lack secondary structure and analogues completely lacking chirality may be synthesized. Further, the use of side chain chirality enables extremely local control over structure, which is often more challenging to achieve via traditional polymerization methods.
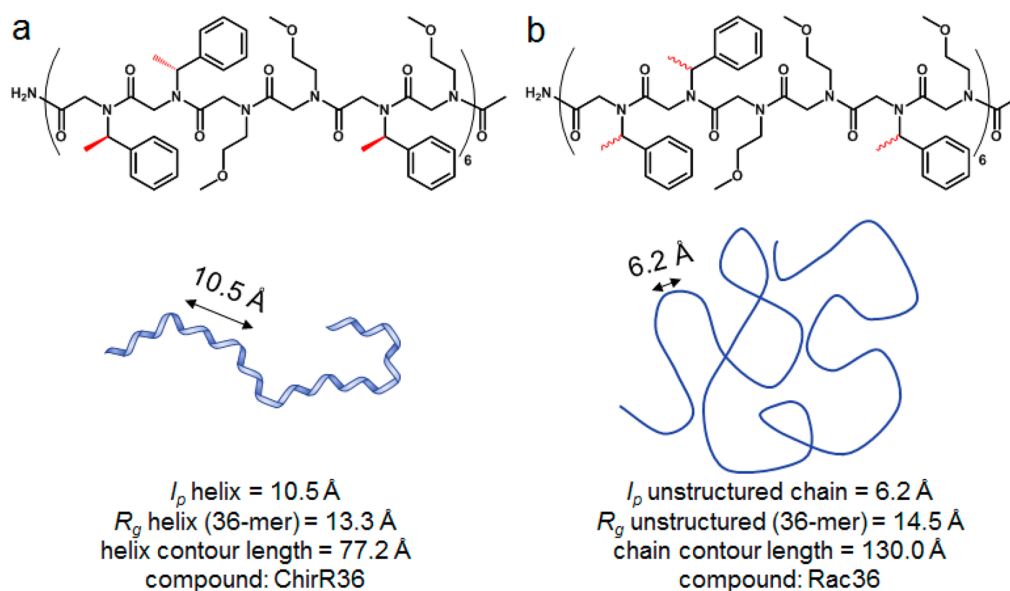
Figure 3. Incorporating bulky side groups with identical *R*-chiralities into the polypeptoid induces a helix (sequence corresponding to "ChirR36" in this paper) (a). Despite the short bending radius of the chain forming the helix, the chain forms a helical secondary structure that has a long persistence length compared to the persistence length of the unstructured chain composed of a racemic mix of side groups (sequence corresponding to "Rac36" in this paper) (b). The helix has a smaller radius of gyration than the unstructured chain. While the helix is relatively stiff, the structure is less space-filling than the unstructured chain. Chirality-inducing bonds are highlighted in red.[36]

While polypeptides can also be synthesized in a sequence-defined manner allowing local control along the chain, the intrinsic hydrogen bonding results in crystallinity which further confounds the direct impact of side chain structure on assembly in the melt. Thus, manipulating secondary structure via the side chain chirality of polypeptoids presents an ideal method for manipulating secondary structure for bulk self-assembly studies

Here, the polypeptoid chain adopts a polyproline I-type helix with *cis* bond conformations preferred from monomer to monomer.[33] Importantly, a preference for an all *cis*-amide bond conformation results in the chain locally having a short bending radius and overall occupying less space. Prior work has directly investigated the chain conformation of these materials in solution via neutron scattering. For 36-unit polypeptoid homopolymers, the helix has an R_g of 13.3 Å (as opposed to the unstructured chain's R_g of 14.5 Å) (Figure 3). However, the favored *cis*-amide bond conformation forms a helix with a persistence length of 10.5 Å, nearly twice that of the unstructured chain (at only 6.2 Å).[36] Importantly, this helical persistence length refers to an effective segment of the helix (which will contain several effective chain units). Further, the contour length of the helix (77.2 Å) is considerably shorter than the contour length of the chain composing it (130.0 Å).[36] This leads to an important feature: the helix will have a more rodlike character than the equivalent unstructured chain ($l_{p,helix}/L_{C,helix} > l_{p,chain}/L_{C,chain}$) (although notably even $l_{p,helix}$ of 10.5 Å is quite short relative to $L_{C,helix}$ of 77.2 Å). Critically, this means that the effective number of segments N_{helix} for the helix will be smaller than the number of segments N_{chain} of the unstructured chain. Further, while the conformational symmetry parameter typically becomes larger with increasing stiffness ($\beta^2 = R_g^2/V$ increases with l_p for a given chain volume V), here β^2 of the helix is actually smaller than β^2 of the unstructured chain for identical volumes V, despite $l_{p,helix} > l_{p,chain}$. Ultimately, this implies that while in a classical coil chain, space-filling properties, resistance to deformation, and local chain stiffness

scale together; here, the helical secondary structure allows a stiffer structure to be created that nonetheless occupies less space and has less configurational freedom. This has important ramifications for self-assembly—in particular, the conformational space occupied and force required to stretch or deform the chain.

Diblock Copolymers Form Cylindrical Morphologies. To directly investigate the effects of the helical versus unstructured chains on block copolymer self-assembly, a series of poly(*n*-butyl acrylate)-*b*-polypeptoid diblock copolymers were synthesized containing an identical poly(*n*-butyl acrylate) block but varying side chain chirality and thus chain properties of the polypeptoid blocks (Figure 4a,b). Coil—coil block copolymers that microphase segregate have a chain conformation that is stretched across the interface; to directly
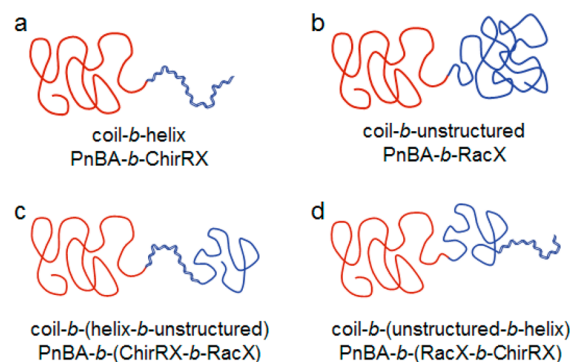

Figure 4. Block copolymers used in this study. Red is poly(*n*-butyl acrylate) while blue is polypeptoid. In (a) the polypeptoid block is entirely helical, while in (b) it is entirely unstructured. In (c) and (d) half of the helical block is helical while the other half is unstructured. In (c) the helical part is located next to the block junction, while in (d) it is located distant from it. Polypeptoids of variable length were used; *X* refers to the number of monomers (18−54).
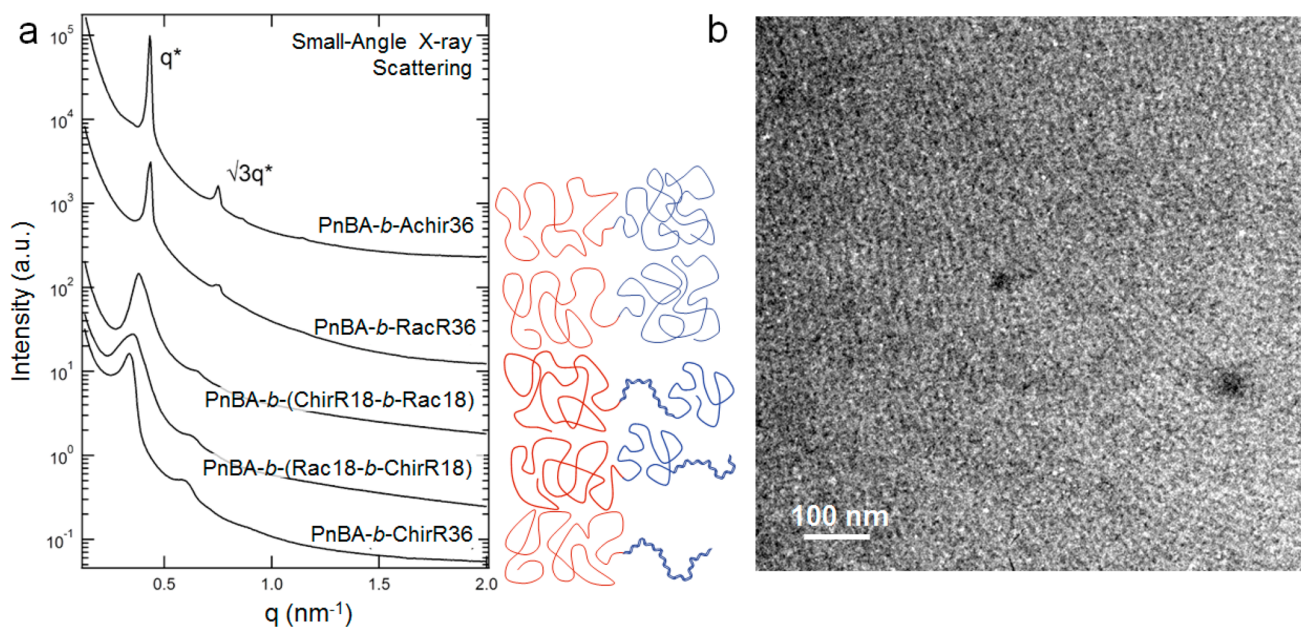
Figure 5. (a) Precise block copolymers show SAXS peaks indicating the formation of hexagonally packed cylinders. These demonstrate shifts in domain spacing in response to changes in polypeptoid chain conformation. Traces are in arbitrary intensity units and offset for clarity. (b) TEM of PnBA-*b*-ChirR54 shows well-ordered cylinders lying down. The sample is in a thin film configuration on a silicon nitride grid; the polypeptoid block is stained with RuO$_4$.

probe this interaction, polypeptoids with both a helical and an unstructured polypeptoid part were synthesized. The helix in these polymers was placed either adjacent to (Figure 4c) or distant from (Figure 4d) the block junction. In particular, due to the condensed structure of the helix, it is expected that the force required to stretch the helix across the interface will be greater than that of the unstructured chain; this will result in a difference in domain size. The synthesized block copolymers (Table 1 and Figure 4) will be referred to as PnBA-*b*-ChirR*X* (PnBA-*b*-ChirR*X*, where *X* is the number of monomers in the polypeptoid block) or PnBA-*b*-unstructured (PnBA-*b*-Rac*X*) for the block copolymers with the homochiral helix-forming and the racemic unstructured polypeptoid block. The block copolymers with the partially helical chain segments will be referred to as PnBA-*b*-(helix-*b*-unstructured) (PnBA-*b*-(ChirR18-*b*-Rac18) or PnBA-*b*-(unstructured-*b*-helix) (PnBA-*b*-(Rac18-*b*-ChirR18)) depending on whether the helical segment is close to the block junction or distant from the block junction, respectively.

All of the described diblock copolymers with polypeptoid blocks at least 36 monomers in length form hexagonally packed cylinders as indicated by the $1:\sqrt{3}:\sqrt{7}$ peak spacing as probed by SAXS and TEM (Figure 5). TEM was performed with a PnBA-*b*-polypeptoid where the polypeptoid consists of a helix-forming 54-mer, for ease of imaging with larger domains. These block copolymers have volume fractions of polypeptoid (f_{peptoid}) from 0.25 for a 36-monomer long polypeptoids to 0.33 for a 54-monomer long polypeptoid; they are all majority poly(*n*-butyl acrylate). The long poly(*n*-butyl acrylate) block creates a preference for the curved interfaces of cylindrical blocks over lamellar morphologies in this regime. Furthermore, this result is also similar to the behavior previously observed for this range of volume fractions in polypeptoid–polystyrene block copolymers.[41] Block copolymers with volume fractions of polypeptoid smaller than 0.25 are disordered. A result of the cylindrical morphology is expected to be that unfavorable

packing interactions arising between stiff, helical polypeptoids will be exaggerated when confined within cylindrical domains relative to those in lamellar domains.

It is also important to consider the role of confinement. Semiflexible chains are especially responsive to local fields and confinement. For example, semiflexible chains with sufficiently strong nematic interactions will align parallel to a surface, with orientational effects that persist to roughly a radius of gyration from the wall.[44,45] While excluded volume effects become extremely important for stiff chains in solution or confined into two dimensions,[45−50] here polypeptoids are studied in the bulk and in net extend perpendicular to the interface. Further, due to the coupling from each block sharing the same interfacial area, the distance between chains varies as each block is stretched. Although the chain conformation is clearly perturbed, it retains significant conformational freedom relative to semiflexible chains confined parallel to surfaces.

Structural Effect of Helix versus Unstructured Chain on Block Copolymer Microdomains. To understand how the helical segment impacts the domain structure, the differences in structure across this series of poly(*n*-butyl acrylate)-*b*-polypeptoid block copolymers are examined. Importantly, across this series of block copolymers the exact same poly(*n*-butyl acrylate) block was used, and the polypeptoid blocks each include precisely the same number and identity of monomers, varying only in side chain chirality. The block copolymers were formed by click chemistry (Supporting Information Scheme 1), allowing this series to be robustly formed. Thus, by examining the changes in domain structure, we are directly probing the impact of secondary structure. It is important to recall that since each block has an identical area per chain at the block copolymer interface and are assumed to be incompressible, that if one block stretches relative to the interface, the other block must also stretch. In the cylindrical geometries described, the cross-sectional area occupied by the polypeptoid cylinder as well as the cross-

sectional area of the PnBA domain will vary as $d*^2$ where $d* = \frac{2\pi}{q*}$ is the domain spacing calculated from the primary peak of SAXS. Detailed calculations of cylinder radius, interdomain spacing, and interfacial area are found in Supporting Information Table 2 (accompanying illustration Supporting Information Figure 8).

In the unstructured block copolymer, the essential physics contributing to the domain structure are similar to those of standard coil−coil block copolymers. In examining the impact of helical versus unstructured polypeptoid blocks, it is expected that the helical block would be more resistant to deformations of chain conformation (in particular, chain stretching at the interface with increasing segregation strength) than the unstructured chain, which would be expected to result in smaller domains. Further, given that the helical polymer occupies less conformational space than the unstructured polymer, the domains were expected to be larger for the unstructured polymer than for the helix, despite the increase in stiffness for the helix. However, instead the block copolymer with the helical block displays a significantly larger domain (approximately a 20% increase in domain size) than the block copolymer with the unstructured chain. This was true across a range of polypeptoid block lengths (number of polypeptoid monomers = 36, 48, and 54) (Figure 6) with identical PnBA
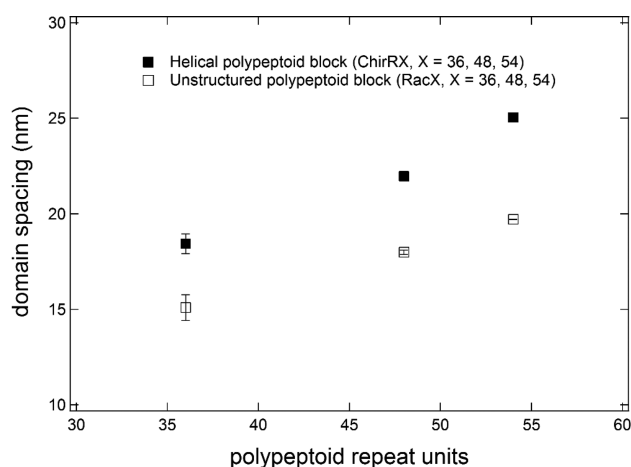
Figure 6. Domain spacing of block copolymers with a chiral (helical) and racemic (unstructured) polypeptoid block, where the polypeptoid blocks have identical numbers of monomers and vary only in side chain chirality. Helical polypeptoids create larger domains for all polypeptoid lengths probed (36, 48, and 54 units). Error in domain size is smaller than marker for X = 48 and X = 54.

blocks. A PnBA-*b*-unstructured diblock copolymer in which the racemic *N*-(1-phenylethyl)glycine was replaced with the achiral *N*-(2-phenylethyl)glycine monomers displayed a nearly identical domain spacing to the racemic case, emphasizing the unstructured nature of the racemic *N*-(±-1-phenylethyl)-glycine-containing polypeptoid. The observed increase in domain size with the helical block may be traced to additional stretching of the PnBA block which occurs due to unfavorable interactions between the PnBA block and the helical block. Alternatively, these changes may be attributed to packing frustrations in the core of the cylinder arising from the stiffer polypeptoid block. Future work will examine similar structures in lamellar nanostructures, where packing frustrations are expected to be minimized as stiff segments can locally align

more readily. However, it is important to realize that the helical block is not a rod; it retains nearly eight persistence lengths per helical 36-mer.

Impact of Helix Placement Relative to Microdomain Interface. To specifically determine the impact of chain stretching at the block copolymer interface versus packing frustrations in the core of the cylindrical microdomains, two structures were designed with the helix-forming section at different parts of the chain (Figures 4c,d and 7c,d). When the
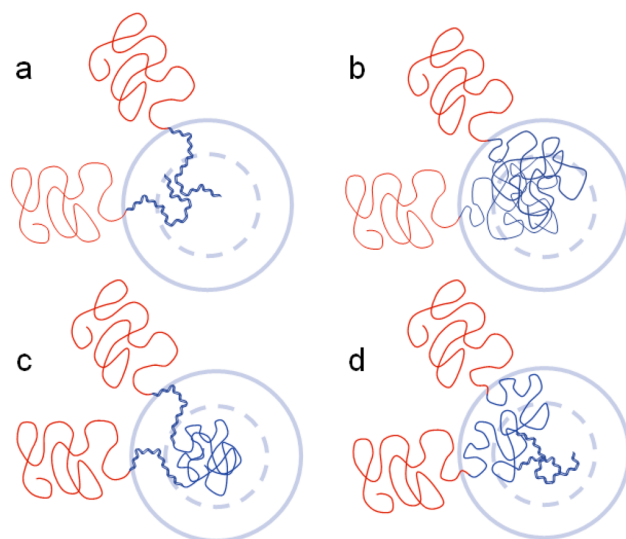
Figure 7. Schematic depicting packing of PnBA-*b*-polypeptoid into hexagonally packed cylinders with varying (a) helical versus (b) unstructured polypeptoid components. (c) and (d) depict the PnBA-*b*-polypeptoid with the helix near the block interface and in the cylinder core, respectively.

helical segment is placed adjacent to the block junction, the block copolymer displays minimal deviation from the unstructured case (Table 1). The unstructured 36-mer results in a domain spacing of 15.1 nm, while when the helix is placed next to the block junction, it expands to only 16.4 nm, not reaching the fully helical polymer's spacing of 18.4 nm. This result indicates that the large increase in domain size cannot arise only from unfavorable interactions between PnBA and the helical secondary structure, as the helix is located proximal to the PnBA in this case. Further, the small domain size likely arises because in this case the helical segment at the edge of the domain spans less space and thus resists stretching, while the unstructured segment of the chain near the center of the domain is able to efficiently fill space. On the other hand, the diblock copolymer with the helix in the domain core and the unstructured chain next to the block junction forms a structure considerably larger than the original. Here, it is believed that this structure arises from chain stretching that is enabled at the edges of domains (which also stretches the PnBA block) in addition to unfavorable packing interactions between helical blocks at the centers of the domains (Figure 7).

Importantly, these observations emphasize how current descriptions of rod−coil interactions and common ways to describe conformational asymmetry do not adequately address the behavior of chain secondary structures. While coil polymers (or any polymer in which the chain itself follows a random walk) will become more space filling with increasing stiffness, secondary structure can cause the chain to deviate. For a helical

polymer, while the overall trajectory of the chain is defined well by the persistence length of the helix, the chain backbone itself travels considerably greater distance (14.2 nm of polypeptoid contour over 10.5 nm of helix contour), thus causing a more condensed conformation (smaller R_g). Essentially, these secondary structures are characterized by nonrandom walk trajectories, where the scaling of space filling and stiff–elastic properties deviate from that of typical coil-like and semiflexible polymers. Here, these helical structures induce larger domains than their unstructured counterparts, primarily arising from interactions in the center of domains, as the helix segments in interfacial regions resist stretching.

Further, helix-containing diblock copolymers display an order–disorder transition at lower temperatures than the equivalent unstructured diblock copolymers (Table 1 and Supporting Information Figures 4–6). For helix-containing PnBA-*b*-ChirR*X*, T_{ODT} = 115 °C for *X* = 36, 136 °C for *X* = 48, and 171 °C for *X* = 54. The analogous block copolymers containing the unstructured block display significantly elevated transition temperatures. For PnBA-*b*-Rac*X*, T_{ODT} = 120 °C for *X* = 36, 150 °C for *X* = 48, and 201 °C for *X* = 54. Each series shows the expected increase in T_{ODT} with increasing *N*, with an increasing disparity between transition temperatures as the size of the polypeptoid block grows. We attribute this difference to the helical structure having fewer available conformations in its condensed chain structure than the equivalent unstructured chain and thus a lower effective *N*. Block copolymer self-assembly occurs under conditions where free energy is minimized by preventing the enthalpic penalties of unlike chain interactions at the expense of losing entropic configurational freedom. Heating above the order–disorder transition temperature, this condition reverses: free energy is minimized by accessing additional configurational freedom, at the expense of allowing unfavorable enthalpic interactions. As a polymer chain's intrinsic configurational freedom decreases (l_p/L_c increases), its effective *N* also decreases, increasing the entropy available through mixing and the T_{ODT}. The lower effective *N* of the helix may also increase the influence of fluctuation effects on the thermodynamics of the transition,[51,52] and the condensed nature of the chain may prevent some of the polypeptoid–PnBA monomer contacts in the disordered state, thus minimizing the enthalpic penalty of disordering. This is in contrast to the result from PS-*b*-PLLA versus PS-*b*-PLA block copolymers where the helical PS-*b*-PLLA phase was observed to be stable to higher temperatures than the PS-*b*-PLA phase.[27] The authors attribute this to stabilized packing of the PLLA chains relative to the PLA; it may be that the bulky side chains of the *N*-(*R*-1-phenylethyl)glycine prevent stabilized packing of these helices. It is important to note that while PLLA readily crystallizes, polypeptoid helices have only been observed to crystallize in oligomers of 4–8 units long following slow (~1 week) crystallization from dilute solution;[38,39] the 24–54-monomer-long oligomers studied here do not display crystallinity. Future studies that decouple the impact of forming a condensed helix on the effective χ will be interesting to understand the relevant thermodynamic parameters controlling the stability of phases containing secondary structures.

This work demonstrates a synthetic approach for producing block copolymers containing helical secondary structures or unstructured chains that are identical apart from side chain chirality. These helical secondary structures form an *all-cis* polyproline I (PPI) type helix, causing the structured chain to be more condensed than the unstructured chain.[36] Similar approaches could examine less dynamic *all-cis* PPI type helixes, such as those induced by naphthalene side groups.[38] A similar approach could be leveraged to examine the opposite extreme: leveraging steric groups and defined sequences that induce the polypeptoid backbone to form either an unstructured chain or an *all-trans* configuration.[53] In this case, the *all-trans* chain is expected to be significantly extended relative to the unstructured chain. Specifically understanding the differences in behavior between the *all-trans* and *all-cis* cases will be important; while in both cases "stiff" structures are formed, the differences in structure are expected to have very different impacts on coordination number as well as the scaling of how well the polymer fills space with increasing chain stiffness. Further, this work has demonstrated the usefulness of leveraging sterics to design sets of materials with chemically identical interactions but dramatically different chain shapes as a way to decouple the impact on self-assembly of chain secondary structure from the impact of chemical interactions between individual repeat units.

■ CONCLUSIONS

Here, we examine the impact of polymer secondary structure on the self-assembly of a series of model PnBA-*b*-polypeptoid block copolymers. The synthetic strategy of using a single PnBA homopolymer for all diblock copolymers, and leveraging truly monodisperse sequence-defined polypeptoids varying only in the chirality of the side chains allows the influence of the secondary structure to be precisely isolated from effects such as polydispersity and backbone or side chain chemical interactions. The helical structure described here prefers the *cis* backbone conformation, thus forming a structure where the helix fills less space than the equivalent unstructured chain, yet is able to form a stiffer structure than it. This structure does not follow the relationships typically associated with descriptions of conformational asymmetry, where local chain stiffness necessarily leads to a more extended structure and increased space-filling properties. Despite this more condensed structure, in this work the helical structure leads to larger domains than the equivalent unstructured chain.

To determine which specific interactions—those at the interface versus those in the core of the cylindrical domains—drive these large domains, polypeptoid sequence control was leveraged to place helical segments at specific positions along the chain. It was found that the resistance of the relatively stiff helix to stretching at the interface inhibits an interfacial contribution to domain size; the majority of the helical contribution to larger domain size appears to originate from packing interactions in the center of cylindrical domains. Future work will examine these block copolymers in lamellar structures, where the role of packing frustrations is expected to be less pronounced than in cylindrical structures. Further, a lower order–disorder transition temperature is observed for the PnBA-*b*-helical diblock copolymers relative to the PnBA-*b*-unstructured diblock copolymers; this is attributed to the lower effective *N* of the condensed polypeptoid helix relative to the unstructured polymer, which increases the entropic gain upon disordering. These deviations of behavior for helical secondary structures from that expected for random walk polymers exhibiting conformational asymmetry emphasizes the importance of developing improved physics for describing the behavior of these systems.

An additional question arises because these helical secondary structures—like many secondary structures—have an intrinsic

handedness. While the system here does not display chirality at larger length scales, hierarchical transfer of chirality has occurred in other block copolymer systems.[27,29] Precise synthetic systems similar to the one described here may be leveraged to address questions of what parameters dominate whether chirality can be transferred across hierarchical length scales. It is expected that synthetically tunable systems with variable pitch, radius, and dynamics can control the strength of cholesteric and other liquid crystalline interactions; ultimately, these are expected to be important parameters for generating new phases, exploring new and unique thermodynamics, and generating new functional materials.

■ ASSOCIATED CONTENT

ⓢ Supporting Information

The Supporting Information is available free of charge on the ACS Publications website at DOI: 10.1021/acs.macromol.8b00055.

> Polypeptoid sequences and secondary structure, block copolymer synthetic scheme, GPC traces, circular dichroism, small-angle X-ray scattering, $1/T$ vs $1/I$ plots for determining T_{ODT}, additional TEM, cylinder radius and interfacial area per chain calculations (PDF)

■ AUTHOR INFORMATION

Corresponding Author

*E-mail: segalman@engineering.ucsb.edu (R.A.S.).

ORCID Ⓞ

Adrianne M. Rosales: 0000-0003-0207-7661

Anastasia L. Patterson: 0000-0003-3875-1195

Ronald N. Zuckermann: 0000-0002-3055-8860

Rachel A. Segalman: 0000-0002-4292-5103

Present Addresses

E.C.D.: John A. Paulson School of Engineering and Applied Sciences, Wyss Institute for Biologically Inspired Engineering, Harvard University, Cambridge, MA 02138.

A.M.R.: McKetta Department of Chemical Engineering, The University of Texas at Austin, Austin, TX 78712.

B.R.: Apple Inc., Cupertino, CA 95014.

Author Contributions

E.C.D. and A.M.R. contributed equally to this work.

Notes

The authors declare no competing financial interest.

■ ACKNOWLEDGMENTS

■ REFERENCES

(1) Wang, Z.-G. 50th Anniversary Perspective: Polymer Conformation—A Pedagogical Review. *Macromolecules* **2017**, *50* (23), 9073−9114.

(2) Bates, F. S.; Schulz, M. F.; Khandpur, A. K.; Forster, S.; Rosedale, J. H.; Almdal, K.; Mortensen, K. Fluctuations, Conformational Asymmetry and Block-Copolymer Phase-Behavior. *Faraday Discuss.* **1994**, *98*, 7−18.

(3) Matsen, M. W.; Bates, F. S. Conformationally asymmetric block copolymers. *J. Polym. Sci., Part B: Polym. Phys.* **1997**, *35* (6), 945−952.

(4) Schulze, M. W.; Lewis, R. M.; Lettow, J. H.; Hickey, R. J.; Gillard, T. M.; Hillmyer, M. A.; Bates, F. S. Conformational Asymmetry and Quasicrystal Approximants in Linear Diblock Copolymers. *Phys. Rev. Lett.* **2017**, *118*, 20.

(5) Almdal, K.; Hillmyer, M. A.; Bates, F. S. Influence of conformational asymmetry on polymer-polymer interactions: An entropic or enthalpic effect? *Macromolecules* **2002**, *35* (20), 7685−7691.

(6) Bates, F. S.; Fredrickson, G. H. Conformational Asymmetry and Polymer-Polymer Thermodynamics. *Macromolecules* **1994**, *27* (4), 1065−1067.

(7) Fredrickson, G. H.; Liu, A. J.; Bates, F. S. Entropic Corrections to the Flory-Huggins Theory of Polymer Blends - Architectural and Conformational Effects. *Macromolecules* **1994**, *27* (9), 2503−2511.

(8) Nagai, K.; Sakajiri, K.; Maeda, K.; Okoshi, K.; Sato, T.; Yashima, E. Hierarchical amplification of macromolecular helicity in a lyotropic liquid crystalline charged poly(phenylacetylene) by nonracemic dopants in water and its helical structure. *Macromolecules* **2006**, *39* (16), 5371−5380.

(9) Hongladarom, K.; Burghardt, W. R. Molecular Alignment of Polymer Liquid-Crystals in Shear-Flow. *Theoretical and Applied Rheology, Vols 1 and 2* **1992**, 537−539.

(10) Shoulders, M. D.; Raines, R. T. Collagen Structure and Stability. *Annu. Rev. Biochem.* **2009**, *78*, 929−958.

(11) Nakano, T.; Okamoto, Y. Synthetic helical polymers: Conformation and function. *Chem. Rev.* **2001**, *101* (12), 4013−4038.

(12) Fujiki, M. Optically active polysilylenes: State-of-the-art chiroptical polymers. *Macromol. Rapid Commun.* **2001**, *22* (8), 539−563.

(13) Nolte, R. J. M. Helical Poly(Isocyanides). *Chem. Soc. Rev.* **1994**, *23* (1), 11−19.

(14) Lam, J. W. Y.; Tang, B. Z. Functional polyacetylenes. *Acc. Chem. Res.* **2005**, *38* (9), 745−754.

(15) Cornelissen, J. J. L. M.; Rowan, A. E.; Nolte, R. J. M.; Sommerdijk, N. A. J. M. Chiral architectures from macromolecular building blocks. *Chem. Rev.* **2001**, *101* (12), 4039−4070.

(16) Yamakawa, H.; Yoshizaki, T. *Helical Wormlike Chains in Polymer Solutions*; Springer: 1997.

(17) Yamakawa, H. Hypothesis on Polymer-Chain Configurations - Helical Wormlike Chains. *Macromolecules* **1977**, *10* (3), 692−696.

(18) Fujii, M.; Nagasaka, K.; Shimada, J.; Yamakawa, H. More on the Model Parameters of Helical Wormlike Chains. *Macromolecules* **1983**, *16* (10), 1613−1623.

(19) Yamakawa, H.; Fujii, M. Statistical-Mechanics of Helical Wormlike Chains 0.4. Persistence Vectors. *J. Chem. Phys.* **1977**, *66* (6), 2584−2588.

(20) Shimada, J.; Yamakawa, H. Statistical-Mechanics of Helical Wormlike Chains 0.5. Distribution Functions. *J. Chem. Phys.* **1977**, *67* (1), 344−352.

(21) Yashima, E.; Maeda, K. Chirality-responsive helical polymers. *Macromolecules* **2008**, *41* (1), 3−12.

(22) Maeda, K.; Takeyama, Y.; Sakajiri, K.; Yashima, E. Nonracemic dopant-mediated hierarchical amplification of macromolecular helicity in a charged polyacetylene leading to a cholesteric liquid crystal in water. *J. Am. Chem. Soc.* **2004**, *126* (50), 16284−16285.

(23) Dellaportas, P.; Jones, R. G.; Holder, S. J. Induction of preferential helical screw senses in optically inactive polysilanes via chiral solvation. *Macromol. Rapid Commun.* **2002**, *23* (2), 99−103.

(24) Majidi, M. R.; Kanemaguire, L. A. P.; Wallace, G. G. Chemical Generation of Optically-Active Polyaniline Via the Doping of Emeraldine Base with (+)-Camphorsulfonic or (−)-Camphorsulfonic Acid. *Polymer* **1995**, *36* (18), 3597−3599.

(25) Prince, R. B.; Barnes, S. A.; Moore, J. S. Foldamer-based molecular recognition. *J. Am. Chem. Soc.* **2000**, *122* (12), 2758−2762.

(26) Chiang, Y. W.; Ho, R. M.; Burger, C.; Hasegawa, H. Helical assemblies from chiral block copolymers. *Soft Matter* **2011**, *7* (21), 9797−9803.

(27) Ho, R. M.; Chiang, Y. W.; Chen, C. K.; Wang, H. W.; Hasegawa, H.; Akasaka, S.; Thomas, E. L.; Burger, C.; Hsiao, B. S. Block Copolymers with a Twist. *J. Am. Chem. Soc.* **2009**, *131* (51), 18533−18542.

(28) Ho, R. M.; Chiang, Y. W.; Lin, S. C.; Chen, C. K. Helical architectures from self-assembly of chiral polymers and block copolymers. *Prog. Polym. Sci.* **2011**, *36* (3), 376−453.

(29) Chiang, Y. W.; Ho, R. M.; Thomas, E. L.; Burger, C.; Hsiao, B. S. A Spring-Like Behavior of Chiral Block Copolymer with Helical Nanostructure Driven by Crystallization. *Adv. Funct. Mater.* **2009**, *19* (3), 448−459.

(30) Zuckermann, R. N.; Kerr, J. M.; Kent, S. B. H.; Moos, W. H. Efficient Method for the Preparation of Peptoids [Oligo(N-Substituted Glycines)] by Submonomer Solid-Phase Synthesis. *J. Am. Chem. Soc.* **1992**, *114* (26), 10646−10647.

(31) Rosales, A. M.; Segalman, R. A.; Zuckermann, R. N. Polypeptoids: a model system to study the effect of monomer sequence on polymer properties and self-assembly. *Soft Matter* **2013**, *9* (35), 8400−8414.

(32) Armand, P.; Kirshenbaum, K.; Falicov, A.; Dunbrack, R. L.; Dill, K. A.; Zuckermann, R. N.; Cohen, F. E. Chiral N-substituted glycines can form stable helical conformations. *Folding Des.* **1997**, *2* (6), 369−375.

(33) Armand, P.; Kirshenbaum, K.; Goldsmith, R. A.; Farr-Jones, S.; Barron, A. E.; Truong, K. T. V.; Dill, K. A.; Mierke, D. F.; Cohen, F. E.; Zuckermann, R. N.; Bradley, E. K. NMR determination of the major solution conformation of a peptoid pentamer with chiral side chains. *Proc. Natl. Acad. Sci. U. S. A.* **1998**, *95* (8), 4309−4314.

(34) Wu, C. W.; Sanborn, T. J.; Zuckermann, R. N.; Barron, A. E. Peptoid oligomers with alpha-chiral, aromatic side chains: Effects of chain length on secondary structure. *J. Am. Chem. Soc.* **2001**, *123* (13), 2958−2963.

(35) Wu, C. W.; Sanborn, T. J.; Huang, K.; Zuckermann, R. N.; Barron, A. E. Peptoid oligomers with alpha-chiral, aromatic side chains: Sequence requirements for the formation of stable peptoid helices. *J. Am. Chem. Soc.* **2001**, *123* (28), 6778−6784.

(36) Rosales, A. M.; Murnen, H. K.; Kline, S. R.; Zuckermann, R. N.; Segalman, R. A. Determination of the persistence length of helical and non-helical polypeptoids in solution. *Soft Matter* **2012**, *8* (13), 3673−3680.

(37) Wu, C. W.; Kirshenbaum, K.; Sanborn, T. J.; Patch, J. A.; Huang, K.; Dill, K. A.; Zuckermann, R. N.; Barron, A. E. Structural and spectroscopic studies of peptoid oligomers with alpha-chiral aliphatic side chains. *J. Am. Chem. Soc.* **2003**, *125* (44), 13525−13530.

(38) Stringer, J. R.; Crapster, J. A.; Guzei, I. A.; Blackwell, H. E. Extraordinarily Robust Polyproline Type I Peptoid Helices Generated via the Incorporation of alpha-Chiral Aromatic N-1-Naphthylethyl Side Chains. *J. Am. Chem. Soc.* **2011**, *133* (39), 15559−15567.

(39) Roy, O.; Dumonteil, G.; Faure, S.; Jouffret, L.; Kriznik, A.; Taillefumier, C. Homogeneous and Robust Polyproline Type I Helices from Peptoids with Nonaromatic alpha-Chiral Side Chains. *J. Am. Chem. Soc.* **2017**, *139* (38), 13533−13540.

(40) Figliozzi, G. M.; Goldsmith, R.; Ng, S. C.; Banville, S. C.; Zuckermann, R. N. Synthesis of N-substituted glycine peptoid libraries. *Methods Enzymol.* **1996**, *267*, 437−447.

(41) Rosales, A. M.; McCulloch, B. L.; Zuckermann, R. N.; Segalman, R. A. Tunable Phase Behavior of Polystyrene-Polypeptoid Block Copolymers. *Macromolecules* **2012**, *45* (15), 6027−6035.

(42) Ilavsky, J. Nika: software for two-dimensional data reduction. *J. Appl. Crystallogr.* **2012**, *45*, 324−328.

(43) Mukherjee, S.; Zhou, G. F.; Michel, C.; Voelz, V. A. Insights into Peptoid Helix Folding Cooperativity from an Improved Backbone Potential. *J. Phys. Chem. B* **2015**, *119* (50), 15407−15417.

(44) Zhang, W. L.; Gomez, E. D.; Milner, S. T. Surface-Induced Chain Alignment of Semiflexible Polymers. *Macromolecules* **2016**, *49* (3), 963−971.

(45) Zhang, W. L.; Gomez, E. D.; Milner, S. T. Using surface-induced ordering to probe the isotropic-to-nematic transition for semiflexible polymers. *Soft Matter* **2016**, *12* (28), 6141−6147.

(46) Semenov, A. N. Adsorption of a semiflexible wormlike chain. *Eur. Phys. J. E: Soft Matter Biol. Phys.* **2002**, *9* (4), 353−363.

(47) Semenov, A. N.; Johner, A. Theoretical notes on dense polymers in two dimensions. *Eur. Phys. J. E: Soft Matter Biol. Phys.* **2003**, *12* (3), 469−480.

(48) Sun, F. C.; Dobrynin, A. V.; Shirvanyants, D.; Lee, H. I.; Matyjaszewski, K.; Rubinstein, G. J.; Rubinstein, M.; Sheiko, S. S. Flory theorem for structurally asymmetric mixtures. *Phys. Rev. Lett.* **2007**, *99* (13), 137801.

(49) Kuznetsov, D. V.; Sung, W. Semiflexible polymers near attracting surfaces. *Macromolecules* **1998**, *31* (8), 2679−2682.

(50) Nam, G. M.; Lee, N. K.; Mohrbach, H.; Johner, A.; Kulic, I. M. Helices at interfaces. *EPL* **2012**, *100* (2), 28001.

(51) Bates, F. S.; Rosedale, J. H.; Fredrickson, G. H. Fluctuation Effects in a Symmetric Diblock Copolymer near the Order-Disorder Transition. *J. Chem. Phys.* **1990**, *92* (10), 6255−6270.

(52) Fredrickson, G. H.; Helfand, E. Fluctuation Effects in the Theory of Microphase Separation in Block Copolymers. *J. Chem. Phys.* **1987**, *87* (1), 697−705.

(53) Stringer, J. R.; Crapster, J. A.; Guzei, I. A.; Blackwell, H. E. Construction of Peptoids with All Trans-Amide Backbones and Peptoid Reverse Turns via the Tactical Incorporation of N-Aryl Side Chains Capable of Hydrogen Bonding. *J. Org. Chem.* **2010**, *75* (18), 6068−6078.